New Polymer Syntheses. 20. Liquid-Crystalline Poly(ester imides) Derived from Trimellitic Acid, α,ω-Diaminoalkanes, and 4,4′-Dihydroxybiphenyl

Hans R. Kricheldorf* and Ralf Pakull

Institut für Technische und Makromolekulare Chemie, Universität Hamburg, Bundesstrasse 45, D-2000 Hamburg 13, FRG. *Received January 22, 1987*

ABSTRACT: Starting from trimellitic anhydride and α,ω-diaminoalkanes with 4–12 methylene groups, a series of nine α,ω-diaminoalkane bis(trimellitimides) were synthesized. Thermal condensation of these diacids with 4,4′-diacetoxybiphenyl yielded the corresponding series of thermotropic homopolyesters. Both DSC measurements and polarizing microscopy show two relatively sharp phase transitions, namely, the crystalline → mesophase transition and the transition from the mesophase to the isotropic phase. Observations under the polarizing microscope and wide-angle X-ray scattering suggest that layered structures exist in the solid state and immediately above the melting points. The melting points and melting enthalpies display the expected odd–even effect, whereas the mesophase → isotropic melt transitions show an almost linear dependence on the length of the aliphatic spacer. In addition to thermogravimetric analyses, thermomechanical analyses were conducted. Due to extremely high rates of crystallization and high degrees of crystallization, the heat-distortion temperatures parallel the melting points (T_m's) and not the glass transition temperatures (T_g's). Therefore heat distortion temperatures in the range of ca. 170–370 °C were found.

Introduction

Many liquid-crystalline main-chain polyesters described in the literature are copolyesters, in particular, copolyesters of 4-hydroxybenzoic acid.[1-6] The properties of copolymers depend on their sequence of the different monomers. In the case of copolyesters the sequences may change in the course of their synthesis of during thermal processing due to transesterification. Hence, the properties of copolyesters may depend on the extent of transesterification, a disadvantage which is necessarily absent in the case of homopolyesters. Also thermotropic homopolyesters, mostly those containing aliphatic spacers, were described in literature.[8-11] From the viewpoint of a technically useful engineering plastic aliphatic spacers entail the shortcoming of lower thermostabilities, relatively low glass-transition temperatures, and correspondingly low heat-distortion temperatures.

The present work was aimed at synthesizing homopolyesters with heat-distortion temperatures above 150 °C, with a thermal stability up to 350 °C, and with moderate melt viscosities. Such a combination of properties was expected from polyesters of *N,N′*-alkane-α,ω-diylbis(trimellitimides) (1) and various bis(phenols). Whereas the present work deals exclusively with homopolymers built up from 4,4′-dihydroxybiphenyl (2), another part of this series will report on similar polyesters containing dihydroxynaphthalenes or substituted and unsubstituted hydroquinones.[12] In this connection a recent patent[13] is worth noting which claims a copolyester mainly consisting of 4-hydroxybenzoic acid, methylhydroquinone, terephthalic acid, and a smaller fraction of diacid **1c** as a fiber-forming material.

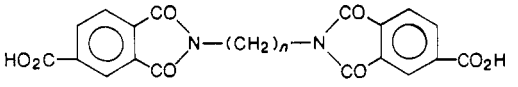

1a, *n* = 4 **f**, *n* = 9
b, *n* = 5 **g**, *n* = 10
c, *n* = 6 **h**, *n* = 11
d, *n* = 7 **i**, *n* = 12
e, *n* = 8

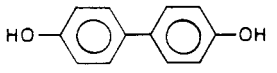

2

Experimental Section

Materials. Trimellitic anhydride was a gift of Bayer AG (Leverkusen, FRG); it was recrystallized from a mixture of toluene and acetic anhydride (mp 164–165 °C). 4,4′-Dihydroxybiphenyl was also a gift of Bayer AG; it was acetylated by means of acetic anhydride in boiling toluene and recrystallized from a mixture of toluene and ligroin (mp 159–160 °C). All α,ω-diaminoalkanes were purchased from Aldrich Co. (St. Louis, MO) and were used without further purification.

***N,N′*-Alkane-α,ω-diylbis(trimellitimides) (1a–i).** An α,ω-diaminoalkane, 0.1 mol, was dissolved in 100 mL of dry dimethylformamide; 0,25 mol of trimellitic anhydride was added and the resulting solution was refluxed for 2 h under stirring. Acetic anhydride, 0.5 mol, was then added and the reaction mixture was refluxed for another 2 h. After it was cooled, the reaction mixture was poured into 1 L of ice-cold water, and the precipitated diacid was isolated by filtration. The products with n = 4–6 (**1a–c**) were recrystallized from dimethylformamide and water. The products with higher n (**1d–i**) were recrystallized from dioxane and water. For yields and properties see Table I.

1,11-Diaminoundecane Dihydrochloride. Tridecanedicarboxylic acid, 0.5 mol, was refluxed with 200 mL of distilled thionyl chloride until the evolution of hydrogen chloride ceased. The diacid chloride was then isolated by distillation in vacuo (yield 92%). This diacid chloride was reacted with 1 mol of trimethylsilyl azide in 500 mL of dry dioxane as described previously for other acid chlorides.[14] The resulting 1,11-diisocyanatoundecane was isolated by distillation in vacuo. This diisocyanate was converted to 1,11-diaminoundecane dihydrochloride by means of dilute hydrochloride acid (yield 93%).

Polycondensations. All condensations were conducted in a cylindrical, round-bottom, glass reactor of ca. 200-mL volume, equipped with gas inlet and oulet tubes and a mechanical stirrer.

A. Condensation of Purified Monomers. A mixture of 50 mmol of an *N,N′*-alkane-α,ω-diylbis(trimellitimide) (**1a–i**) and 50 mmol of 4,4′-diacetoxybiphenyl was heated under a slow stream of nitrogen for 15 min at 250 °C, for 15 min at 280 °C, and for 60 min at 320 °C, whereby most acetic acid was removed. When the aliphatic spacer contained more than eight methylene groups, heating was continued for 1 h at 320 °C in vacuo. In the case of shorter spacer (**1a–e**) the temperature was gradually raised to 340 °C over a period of 1 h, and during the last 30 min vacuum was applied. After cooling the poly(ester imides) were isolated mechanically, because most of them are insoluble in all common solvents.

B. One-Pot Procedure. Trimellitic anhydride, 100 mmol, and 50 mmol of an α,ω-diaminoalkane (or its hydrochloride) were molten in the aforementioned glass reactor under stirring. After a condensation period of 45 min, vaccum was applied for 15 min to remove water completely. 4,4′-Diacetoxybiphenyl, 50 mmol, was then added and the condensation continued as described above.

Measurements. The viscosities were measured with an automated Ubbelohde viscosimeter thermostated at 20 °C. Solutions of 100 mg of polymer in 50 mL of a 1:4 (by volume) mixture of

0024-9297/88/2221-0551$01.50/0 © 1988 American Chemical Society

Table I
Yields and Properties of *N,N'*-Alkane-α,ω-diylbis(trimellitimides) (1a–i)

compd	*n*	yield, %	mp °C	elem formula (secd. wt)	elem anal.; calcd, found C	H	N
1a	4	69	343–345	$C_{22}H_{16}N_2O_6$ (436.4)	60.55, 60.29	3.70, 3.78	6.42, 6.69
1b	5	77	244–248	$C_{23}H_{18}N_2O_6$ (450.4)	61.33, 61.50	4.03, 4.02	6.22, 6.26
1c	6	67	321–322	$C_{24}H_{20}N_2O_6$ (464.4)	62.07, 62.07	4.40, 4.34	6.16, 6.03
1d	7	60	220–222	$C_{25}H_{22}N_2O_6$ (478.4)	62.76, 62.60	4.63, 4.70	5.85, 5.79
1e	8	78	242–243	$C_{26}H_{24}N_2O_6$ (492.5)	63.41, 63.51	4.91, 5.06	5.68, 5.88
1f	9	95	204–205	$C_{27}H_{26}N_2O_6$ (506.5)	64.03, 64.01	5.17, 5.25	5.53, 5.73
1h	10	91	221–224	$C_{28}H_{28}N_2O_6$ (520.5)	64.61, 69.69	5.42, 5.55	5.48, 5.46
1i	12	91	210–211	$C_{30}H_{32}N_2O_6$ (548.6)	65.68, 65.74	5.88, 5.87	5.11, 5.30

Table II
Yields and Properties of Poly(ester imides) Prepared from *N,N'*-Alkane-α,ω-diylbis(trimellitimides) and 4,4'-Diacetoxybiphenyl

compd	*n*	yield, %	η_{inh}[a]	T_g,[b] °C	T_{m_1},[b] °C	T_{m_2},[b] °C	LC[c] phase, °C	elem formula (mol wt)	elem anal.; calcd, found C	H	N
3a	4	90.6	insol	126	393	dec	398–467	$C_{34}H_{22}N_2O_8$ (586.56)	69.92, 68.29	3.78, 3.79	4.78, 5.03
3b	5	95.0	0.79	147	356	dec	352–441	$C_{36}H_{24}N_2O_8$ (600.59)	70.00, 69.93	4.03, 4.05	4.66, 4.73
3c	6	93.0	insol	133	361	dec	370–439	$C_{36}H_{26}N_2O_8$ (614.62)	70.35, 69.84	4.26, 4.60	4.56, 4.93
3d	7	92.5	1.23	117	290	408	297–429	$C_{37}H_{28}N_2O_8$ (628.64)	70.69, 70.60	4.49, 4.56	4.46, 4.65
3e	8	92.0	insol	n.b.	339	414	349–413	$C_{38}H_{30}N_2O_8$ (642.67)	71.02, 70.25	4.71, 4.74	4.36, 4.48
3f	9	88.0	1.15	n.b.	246	406	245–400	$C_{39}H_{32}N_2O_8$ (656.70)	71.33, 71.21	4.91, 5.01	4.27, 4.42
3g	10	93.0	insol	n.b.	310	404	320–390	$C_{40}H_{34}N_2O_8$ (670.72)	71.63, 71.54	5.11, 5.18	4.18, 4.22
3h	11	79.7	0.84	97	245	370	250–380	$C_{41}H_{36}N_2O_8$ (684.75)	71.98, 72.27	5.39, 5.52	4.09, 4.39
3i	12	91.5	insol	n.b.	297	386	300–386	$C_{42}H_{38}N_2O_8$ (698.78)	72.19, 72.17	5.48, 5.63	4.01, 3.97

[a] Measured with c = 2 g/L in a 4:1 mixture (by volume) of dichloromethane and trifluoroacetic acid. [b] From DSC measurements conducted at a heating rate of 20 °C/min. [c] As observed under the polarizing microscope.

trifluoroacetic acid and dichloromethane were used in all cases.

The ^{13}C NMR spectra were obtained on a Bruker AM-360 FT spectrometer at ca. 20 °C. Solutions of 200 mg of polymer in 2 mL of trifluoroacetic acid were measured in 10-mm-o.d. sample tubes equipped with a coaxial 4-mm tube containing TMS and dioxane-d_8. A pulse width of ca. 45° was used together with a relaxation delay of 2 s and a digital resolution of 32K data points/18 000-Hz spectral width.

The DSC traces were measured with a Perkin-Elmer DSC-4 at a heating rate of 20 °C/min in aluminum pans.

The thermomechanical analyses were conducted with a Perkin-Elmer TMS-2 under a pressure of 1 kg/mm^2 at a heating rate of 5 °C/min. Thin films with a thickness of ca. 0.5 mm were prepared at ca. 340 °C. The thermogravimetric analyses were obtained on a Perkin-Elmer TGS-2 at a heating rate of 10 °C/min in air.

The wide-angle X-ray scattering (WAXS) curves were measured with a powder diffractometer "Siemens D-500" by means of Cu Kα radiation and a Ni filter. For the set of slits between radiation source and scintillation detector, angles of 10°, 1°, 0.1°, and 0.5° were chosen. The diagrams were recorded in steps of ϑ = 0.1° with a radiation time of 20 s/data point.

Resuits and Discussion

Syntheses. The *N,N'*-alkane-α,ω-diylbis(trimellitimides) **1a–g,i** were synthesized from the corresponding α,ω-diamines and trimellitic anhydride. The complete cyclization of the intermediate amino acids was achieved by acetic anhydride. The diacid **1c** has already been described in literature.[15–17] It was used for syntheses of various poly(amide imides) and poly(ester imides) that do not form liquid-crystalline (LC) phases. Furthermore, the diacids **1a** and **1b** were claimed in the aforementioned patent[13] as components of fiber-forming thermotropic copolyesters of 4-hydroxybenzoic acid, yet their properties were not described. Therefore, melting points and elemental analyses of all diacids used in this work were determined and summarized in Table I.

The recrystallized diacids **1a–g,i** were condensed with 4,4'-diacetoxybiphenyl in the presence of magnesium acetate. The reaction temperature was gradually raised from 250 or 320 °C. Only in the case of short aliphatic spacers (n < 8) the final reaction temperature was raised to 340 °C, because the corresponding poly(ester imides) **3a–e** rapidly solidified at temperatures below 320 °C. All poly(ester imides) were isolated as yellowish or brownish hard crystalline materials; their yields and properties are summarized in Table II.

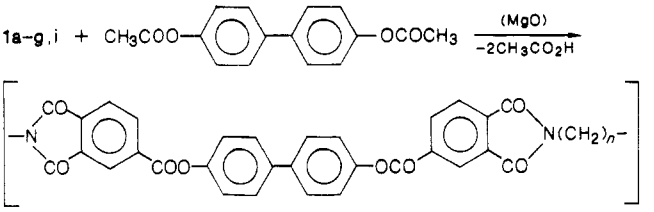

(1)

Because 1,11-diaminoundecane was not commercially available, the synthesis of the corresponding poly(ester imide) **3h** was conducted in a slightly different way. Tridecanedecarboxylic acid was converted to the diacid chloride which was reacted with trimethylsilyl azide (eq 2) as described previously for other acid chlorides.[14] The

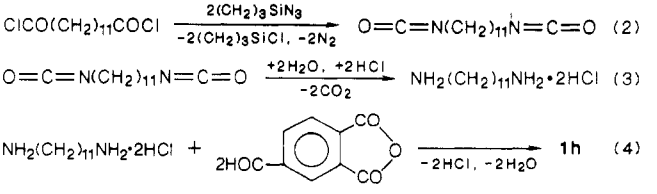

resulting 1,11-diisocyanatoundecane was hydrolyzed with dilute hydrochloric acid (eq 3). The hydrochloride of 1,11-diaminoundecane was condensed with trimellitic anhydride (eq 4) and the condensation was continued by addition of 4,4'-diacetoxy biphenyl without isolation of monomer **1h**. In this "one-pot" procedure poly(amide imide) segments might be formed. However, when the "one-pot" procedure poly(amide imide) was used for the synthesis of **3i** the resulting polymer was identical with that prepared in a stepwise manner. Furthermore, the ^{13}C

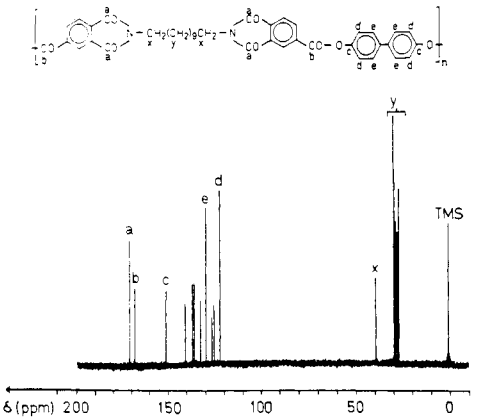

Figure 1. ^{13}C NMR spectrum, 90.5 MHz, of the poly(ester imide) **3h**, prepared from 1,11-diaminoundecane dihydrochloride trimellitic anhydride and 4,4'-diacetoxybiphenyl in an "one-pot procedure".

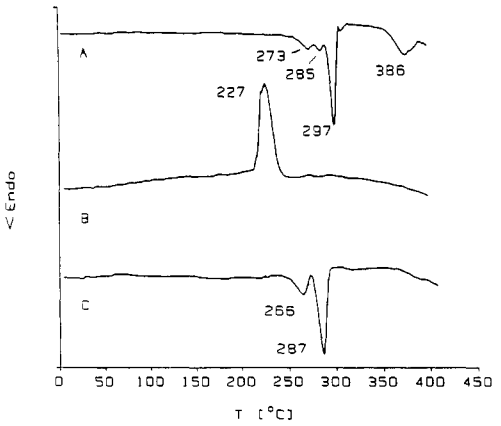

Figure 2. DSC traces (heating and cooling rates, 20 °C/min) of the poly(ester imide) **3i** (n = 12): (A) first heating; (B) cooling; (C) second heating.

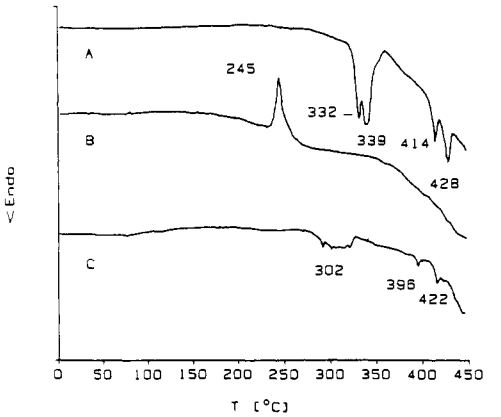

Figure 3. DSC traces (heating and cooling rates, 20 °C/min) of the poly(ester imide) **3e** (n = 8): (A) first heating; (B) cooling; (C) second heating.

NMR spectrum of **3h** only exhibits two carbonyl signals as expected for the ester imide structure (Figure 1). A comparison of this spectrum with that of poly(amide imides) prepared from trimellitic anhydride and 1,12-diaminododecane or n-butylamine justifies this conclusion. In this connection it must be mentioned that this "one-pot" procedure is not useful for poly(ester imides) with short aliphatic spacers ($n \leq 6$) because the intermediately formed diacids (**1a–c**) solidify at temperatures <320 °C (Table I).

Unfortunately, no information was available on those poly(ester imides) with even numbers of methylene groups because they are insoluble in all common solvents that do not degrade ester groups. All poly(ester imides) with odd numbers of methylene groups above 5 are soluble in hexafluoroisopropyl alcohol and in the mixtures of trifluoroacetic acid (TFA) and dichloromethane or chloroform. The relatively high inherent viscosities (Table II) suggest that the molecular weights are high enough for potential technical applications. In agreement with this conclusions, tough films could be cast from solution and fibers drawn from the melt.

DSC Measurements. The poly(ester imides) **3a–i** were subjected to DSC measurements at a heating rate of 20 °C/min. In all cases a distinct, sharp endotherm was detectable below 400 °C, indicating the transition from the crystalline to liquid-crystalline phase (Figure 2). Only polymer **3e** (n = 8) displayed two sharp closely neighboring peaks (Figure 3). These peaks coalesce into one broader endotherm on repreated heating (Figure 3), and thus, may represent crystallites of different size. Upon cooling from the melt the DSC traces of all poly(ester imides) exhibit an exotherm below 300 °C which represents the crystallization process (Figure 2 and 3). This exotherm is detectable regardless of the cooling rate, indicating that the rates of crystallization are high. Due to these high rates of crystallization, amorphous materials were never obtained upon cooling in the DSC machine. Only quenching from the melt by means of liquid nitrogen yielded more or less amorphous samples so that in most cases glass-transition temperatures (T_g's) could be measured (Table II). However, those poly(ester imides) with long spacers crystallized so rapidly (with the exception of **3h**) that even after quenching T_g's were not measurable. The T_g's listed in Table II show a rough tendency to increase with decreasing length of the spacer. This tendency is reasonable because the segmental mobility decreases in the same order, and obviously, the rates of crystallization follow the same pattern. In this connection it is noteworthy that the WAXS synchrotron radiation measurements (see below) indicate almost complete crystallization within 1 min.

In separate DSC measurements calibrated with indium, the melting enthalpies at T_{m_1} were determined. The values listed in Table III were calculated from the peak areas of the endotherms in the first heating traces. Values obtained from the second heating curves were constantly lower, obviously, because heating to temperatures around 400 °C entailed partial degradation (see Table III and discussion below). Since the degrees of crystallinity were unknown, the enthalpies of Table III do not represent the absolute values of 100% crystalline materials. Nonetheless, these enthalpies display two interesting tendencies. First, they show an odd–even effect, and second, they increase with decreasing lengths of the spacers in good agreement with the heights of the melting points according to the equation: $T_{m_1} = \Delta H_1/\Delta S_1$. In this connection it is worth noting that, for instance, aliphatic polyamides or polyimides or polyesters and poly(alkylene terephthalates) show increasing melting enthalpies with increasing molecular weight of the monomer units, because all groups of the monomer unit make similar energetic contributions due to their van der Waals forces. The opposite trend observed for **3a–h** suggests that the interchain interactions of the methylene groups are significantly lower than those of the mesogenic group, which possesses strong dipoles.

The DSC traces of poly(ester imide) with long spacer ($n \geq 8$) also display a second endotherm (T_{m_2}) at temperatures close to 400 °C which (with exception of **3e**) is broader than that of T_{m_1} (Figure 2). In the case of shorter spacers, rapid thermal degradation prevents observation

Table III
Heat Distortion Temperature and Thermostability of Poly(ester imides) 3a–i

compd	n	T_{m_1},[a] °C	ΔH_{m1},[b] kJ/mol	heat-distortion[c] temp, °C		temp with following wt loss[d]			
						1%	5%	10%	20%
3a	4	393	25.2 ± 0.4	390	370	366	430	449	463
3b	5	356	15.0 ± 0.5	317	300	372	425	441	456
3c	6	361	23.4 ± 0.5	257	206	335	401	424	444
3d	7	290	9.3 ± 1.0	255	245	366	418	437	453
3e	8	341	20.5 ± 1.0	335	287	360	404	425	444
3f	9	246	6.7 ± 0.4	235	225	357	405	434	462
3g	10	310	12.1 ± 0.5	320	279	338	415	441	461
3h	11	245	6.2 ± 0.5	240	143				
3i	12	297	14.2 ± 0.7	245	165				

[a] Minimum of the melting endotherm in the DSC trace. [b] Peak area of the DSC endotherm of the first heating curve calculated per mole of repeat unit. [c] Measured at a heating rate of 5 °C/min under a pressure of 0.05 kg/mm² (first column) or 1 kg/mm² (second column). [d] Thermogravimetric analyses conducted at a heating rate of 10 °C/min in air.

of the second endotherm which indicates the transition from the anisotropic to the isotropic melt. Quantitative measurements of samples **3e,f,i** yielded transition enthalpies of ca. 6.0, 3.6, and 3.0 kJ/mol. A comparison of these enthalpies with those of the melting point T_{m_1} (Table III) demonstrates that the phase transition to the isotropic melt involves weaker intermolecular forces than the solid smectic transition. However, when the mesogenic group is smaller the enthalpy of the smectic isotropic transition increases at the expense of the solid smectic transition as demonstrated in future parts of this series.

Polarization Microscopy. Observation under the polarizing microscope confirms the above interpretation of the DSC curves (Table II). At T_{m_1} anisotropic melts are formed with a granular texture that fit better with published textures of smectic low molecular weight mesogenes[18] or with the so-called broken focal conic texture reported for smectic melts of various polyesters.[7] This granular texture is clearly distinguishable from the "schlieren textures" of nematic phases that were found for random copolyesters of 4-hydroxybenzoic acid such as PET/PHB copolyester[1,2] or copolyesters of β-(4-hydroxyphenyl)propionic acid.[7] Furthermore, copolymers of diacid **1i**, hydroquinone, and 4-hydroxybenzoic acid were prepared by thermal condensation and investigated by microscopy with crossed polymerizers (described in a future part of this series). These random copolyesters exhibit the typical "threadened schlieren texture" of a nematic phase (published, for example, in Figure 12 of ref 11). Thus, the microscopic characterization of poly(ester imides) **3a–i** gives clear evidence for the existence of smectic melts, a result that agrees well with the regular primary structure of these homopolyesters.

When the anisotropic melt is heated to the transition into the isotropic phase, no significant change of the texture is observable; in other words a smectic–nematic transition was never observable. When a plot of T_{m_1} and T_{m_2} of poly(ester imides) **3a–i** versus the spacer length (Figure 4) is compared to that of the polyesters **4a–i**[19] (Figure 5), the following observations are worth noting. First, both melting points T_{m_1} and T_{m_2} are significantly higher. Second, the odd–even effect of T_{m_1} is more pronounced in the case of **3a–i**, in contrast to T_{m_2} which displays a strong odd–even effect only in the case of **4a–i**.

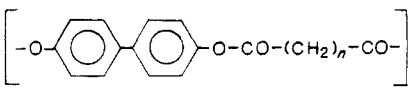

4a–i

Third, the mesongenic phase of **3a–i** covers a broader temperature range. This comparison clearly demonstrates that the imide groups of **3a–i** are an important component of the mesogenic group.

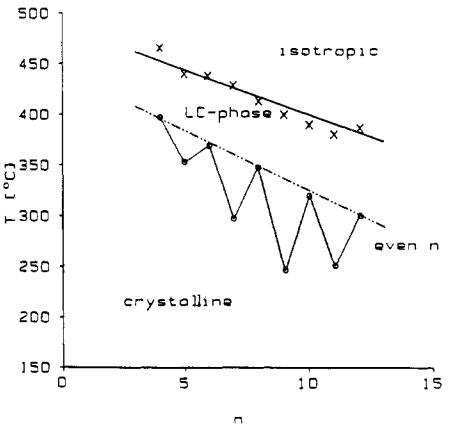

Figure 4. Plot of melting points (T_{m_1}) and anisotropic–isotropic transitions versus number of methylene groups in the aliphatic spacers of **3a–i**.

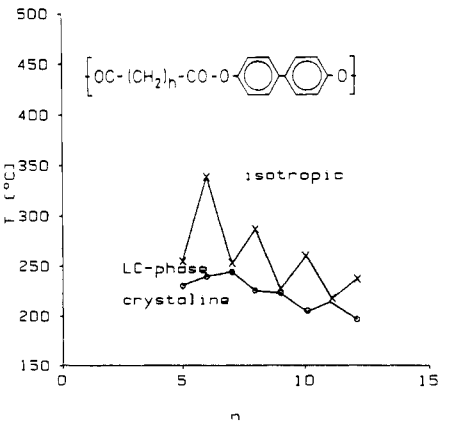

Figure 5. Plot of melting points (T_{m_1}) and anisotropic–isotropic transitions (T_{m_2}) versus the number of methylene groups in the spacer of polyesters **4a–i**.

WAXS Measurements. In order to obtain more information on the supermolecular order of the poly(ester imides) **3a–i** in the solid state and in the anisotropic melt, WAXS measurements were conducted under various conditions. In a first series of measurements powder patterns of all polymers were recorded at room temperature. Characteristic for these powder patterns is a group of sharp reflections between $\vartheta = 1°$ and 7° and a broader signal (in some cases with shoulder) at $\vartheta = 9.7 - 10.0°$ (Figure 6). The latter reflection represents the lateral packing of the chains with a distance of 4.5 ± 0.1 Å. This reflection was found in all powder patterns of LC poly(ester imides) investigated so far (see future parts of this series), and it is present in the WAXS patterns of many LC polyesters.[1,7,19,20] The $\delta = 10°$ reflection indicates a

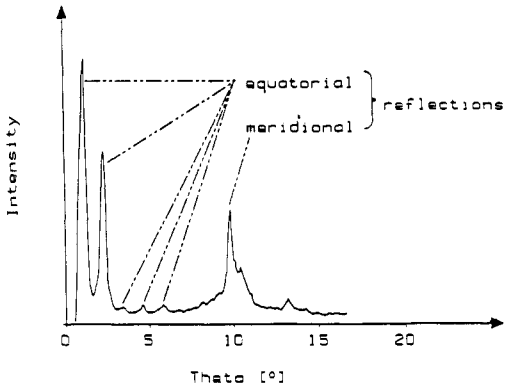

Figure 6. WAXS powder pattern of partially oriented crude poly(ester imide) **3i** (n = 12), as obtained by slow cooling of the stirred reaction mixture.

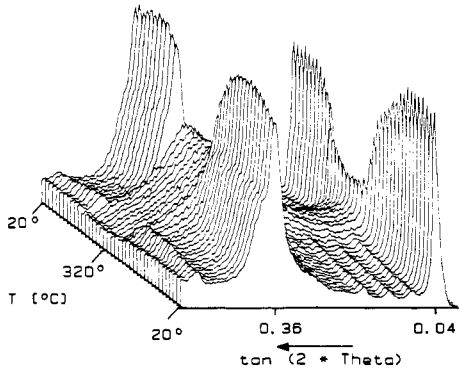

Figure 7. WAXS synchrotron radion measurements of poly(ester imide) **3i** (n = 12) conducted with a heating and cooling rate of 20 °C/min between 20 and 320 °C.

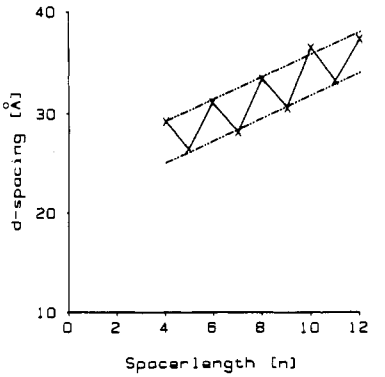

Figure 8. Plot of d-spacings calculated from the small-angle reflection in the WAXS powder patterns of poly(ester imides) **3a–i** versus the number of methylene groups in the aliphatic spacers.

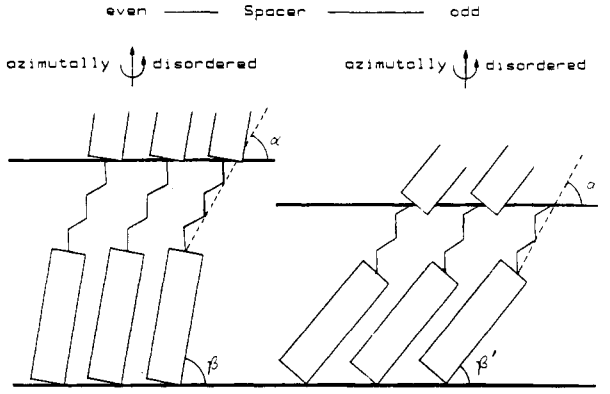

Figure 9. Scheme of the supermolecular structure of the poly(ester imides) **3a–i**.

hexagonal packing of chains, when a splitting into two reflections—typical for a orthorhombic cell—is not detectable upon heating.

All small-angle reflections (ϑ = 1–7°) of one sample correspond to the same d-spacing. Obviously, they are the first and higher order reflections of a layered supermolecular structure with identical d-spacings between all layers when WAXS patterns are measured by means of synchtrotron radiation at temperatures up to T_{m_2} (Figure 7). The second-order reflection remains observable even in the anisotropic melt (the first-order reflection was not measurable under these conditions). This result confirms the microscopic characterization of the ansisotropic melt as a smectic phase. The disappearance of the higher order reflections above T_{m_1} suggests that the layer plane of the smectic phase is less perfect than those of the crystalline state. Furthermore, the conspicuous broadening of the δ = 10° reflection indicates that the order of the lateral packing is significantly reduced in the melt. Above T_{m_1} the mesogens presumably obtain freedom of rotation in agreement with the relatively high enthalpy change at T_{m_1} (compared to T_{m_2}).

The d-spacings of the layer plane calculated from the small reflections measured at room temperature fall into the range 25–40 Å. These d-spacings correspond to the lengths of the repeat units, when a tilted array relative to the layer planes is assumed. Two observations are of particular interest. First, the d-spacings parallel the lengths of the spacers (Figure 8) and the slopes of these plots are identical for polymers with even and polymers with odd spacers. Second, the d-spacings display a pronounced odd–even effect. The first observations suggest that the tilt angle of the spacers relative to the layer planes (α in Figure 9) is nearly identical for polymers with even and odd spacers. From the slope of 2.25 Å per ethylene unit (Figure 8) and from the pitch of an ethylene unit in the zigzag chain of crystalline polyethylene (2.53 Å), a tilt angle $\alpha = 63 \pm 2°$ may be calculated. This angle should be considered as a minimum value, because the conformation of the spacers possible deviates from a perfectly planar zigzag conformation (see below). Yet, any conformation which shortens the effective spacer length increases the tilt angle α. A reasonable calculation of the tilt angles of the mesogenic groups (β on β' in Figure 9) was not feasible because the true conformation of the mesogenic groups was unknown. However, the shorter d-spacings of the polymers with odd spacers indicate that the tilt angles of their mesogenes are significantly smaller than those of the polymers with even spacers ($\beta' < \beta$ in Figure 9). The difference of the d-spacings of polymers with even and odd spacers amounts to 4.1 ± 0.2 Å, a value which cannot be explained by different conformations of the even and odd spacers. A qualitative representation of these results is given in the scheme of Figure 9.

All attempts to determine the tilt angles of the repeating units from fiber patterns of the poly(ester imides) **3a–i** failed because all reflections appeared on the equator and/or the meridian. Obviously, the scattering effects of the tilt angles in subsequent layers cancel each other due to azimuthal disorder. Analogous X-ray results were first reported by Leadbetter and Norris[21] for low molecular weight mesogenes (Figure 3b in ref 21). Furthermore, it is noteworthy that the fiber patterns of poly(ester imides) with even and odd spacers may look different. In the case of **3i** (n = 12) the δ = 10° reflection appeared on the meridian and the small-angle reflections on the equator (Figure 6). Obviously the layer planes are parallel the fiber axis, whereas the chain axis is aligned perpendicular to the

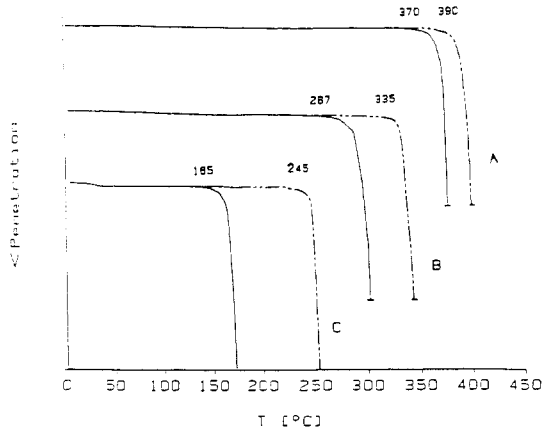

Figure 10. Thermomechanical analyses (penetration of foils) measured at a heating rate of 5 °C/min under a pressure of 1 kg/mm^2 (or 0.05 kg/mm^2, dotted lines): (A) **3a** (n = 4); (B) **3e** (n = 8); (C) **3i** (n = 12).

fiber axis. This orientation is exactly opposite to that found for poly(ester imides) prepared from the diacids **1a–i** and hydroquinone (see subsequent paper) or for poly(ester imides) prepared from trimellitic acid, ω-amino acids, and various bisphenols).[22] Nonetheless, also parallel orientations of smectic layers and fiber axis were reported in several cases[23–25] and, thus, do not represent any extraordinary morphology.

The fiber pattern of polymer **3f** (n = 9) displays the ϑ = 10° reflection on the equator and the small-angle reflections on both the meridian and the equator in nearly equal intensities. This unexpected result cannot be interpreted at the current state of research; yet further X-ray studies are in progress. Nonetheless, the fiber patterns of **3f** and **3i** confirm that the chain packing of poly(ester imides) with even and odd spacers is different. Regardless of the exact nature of this chain packing, it may be emphasized that the crystal lattice of odd-membered spacer is energetically less favorable because the melting points are lower, the melting enthalpies at T_{m_1} are lower, and the solubility in organic solvents is significantly higher.

Thermomechanical Properties and Thermostability. With regard to any application as thermotropic engineering plastic, the heat-distortion temperature (HDT) is an important property. Therefore, the poly(ester imides) **3a–i** were subjected to thermomechanical analyses at two different pressures. The values listed in Table III show that the breakdown of the mechanical resistance under low pressure occurs at temperatures where the melting process sets in. When the pressure is increased by a factor of 20 (comparable with the Vicat-A test) the heat-distortion temperatures decrease, yet with the exception of **3h,i** the HDTs still remain close to the melting temperature. In the case of **3h,i**, the poly(ester imides) with the highest segmental mobility, a significant decrease of the HDT was found, yet even here the values are considerably higher than T_g (Table III). Despite rapid cooling (ca. 300 °C/min) the foils pressed at 360 °C do not display any indication of a glass transition in their TMA curves (Figure 10). These results demonstrate again that the poly(ester imides) **3a–i** possess high rates of crystallization and high degrees of crystallinity.

The observed curves of HDT also suggest that the crystallites form a coherent matrix with a morphology where the amorphous phase is dispersed in the voids of the crystalline domains. Such a morphology is less frequently found among crystalline polymers than the alternative situation, namely, crystallites dispersed in a coherent amorphous matrix. A typical example of the latter

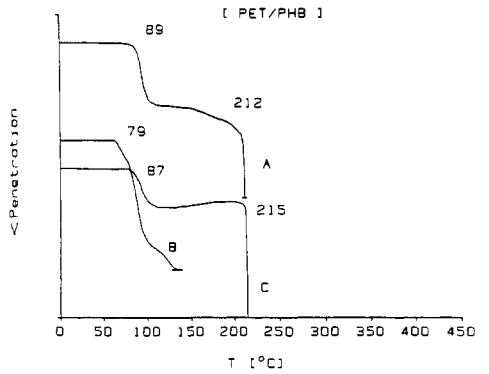

Figure 11. Thermomechanical analyses (penetration method measured at a heating rate of 5 °C/min under a pressure of 1 kg/mm^2: (A) PET/PHB 60:40 mol %; (B) PET/PHB 50:50 mol %; (C) PET/PHB 30:70 mol %.

morphology is represented by copolyesters of poly(ethylene terephthalate) and 4-hydroxybenzoic acid (PET/PHB). As demonstrated in Figure 11, the HDT of these LC copolyesters is as low as the T_g (in the range 80–100 °C) over a broad range of composition, despite the relatively short aliphatic spacers. Low heat-distortion temperatures were also reported for a class of thermotropic polyesters with a regular sequence of aromatic mesogens and aliphatic spacers (Figure 13 in ref 6).

Finally, the thermal stability of the poly(ester imides) was characterized by means of thermogravimetrical analyses conducted at a heating rate of 10 °C/min in air. Slight degradation, only detectable upon prolonged heating at constant temperature, begins in the range 330–340 °C. However, at these temperatures degradation is so slow that mechanical processing is feasible up to temperatures of ca. 360 °C. Rapid degradation begins above 400 °C (Table III). Both thermostability and flammability of **3a–i** are certainly lower than those of fully aromatic polyesters.

Nonetheless, the poly(ester imides) described in this work possess an interesting combination of several useful properties. The mobility of the LC melt observed under the microscope and the good stirrability observed in the course of the syntheses indicate a relatively low melt viscosity. The temperature range of the LC phase is broad enough and the thermostability is high enough to enable any kind of processing up to temperatures around 360 °C. Furthermore, high rates of crystallization, high degrees of crystallization, and a favorable morphology enable heat-distortion temperatures far above the glass-transition temperature.

Acknowledgment. We thank Dr. H. Biskup (Bayer AG Uerdingen, FRG) for the thermogravimetrical analyses, we thank Dipl.-Phys. S. Buchner (University of Hamburg) for the WAXS synchrotron radiation measurements, and we thank the BMFT and the BAYER AG (Uerdingen, FRG) for financial support.

Registry No. **1a**, 111822-73-2; **1b**, 76860-19-0; **1c**, 4649-28-9; **1d**, 76860-20-3; **1e**, 52454-86-1; **1f**, 76819-66-4; **1**, 76860-18-9; **1i**, 52644-69-6; **3a** (copolymer), 111847-68-8; **3a** (SRU), 111847-75-7; **3b** (copolymer), 111847-69-9; **3b** (SRU), 111847-76-8; **3c** (copolymer), 111847-70-2; **3c** (SRU), 111847-77-9; **3d** (copolymer), 111847-71-3; **3d** (SRU), 111847-78-0; **3e** (copolymer), 111847-72-4; **3e** (SRU), 111847-79-1; **3f** (copolymer), 111847-73-5; **3f** (SRU), 111847-80-4; **3g** (copolymer), 107185-81-9; **3g** (SRU), 107227-43-0; **3h** (copolymer), 111847-74-6; **3h** (SRU), 111847-81-5; **3i** (copolymer), 111868-84-9; **3i** (SRU), 111847-82-6.

References and Notes

(1) Jackson, W. J.; Kuhfuss, H. F. *J. Polym. Sci., Polym. Chem. Ed.* **1976**, *14*, 2042.
(2) Jackson, W. J. *Br. Polym. J.* **1980**, *12*, 154.

(3) Volksen, W., Jr.; Lyerla, R., Jr.; Economy, J.; Dawson, B. *J. Polym. Sci., Polym. Chem. Ed.* **1983**, *21*, 2249.
(4) Calundann, G. W. Ger. Offen. 2 721 780, Nov 24, 1977, to Celanese Corp.; *Chem. Abstr.* **1978**, *88*, 74883d.
(5) Calundann, G. W.; Charbonneau, L. F.; East, A. J. U.S. Patent 4 351 917, April 6, 1981, to Celanese Corp.
(6) Huynh-Ba, G.; Cluff, E. F. In *Polymer Liquid Crystals*; Blumenstein, A., Ed; Plenum: New York–London, 1985; p 217 ff.
(7) Kricheldorf, H. R.; Conradi, A. *J. Polym. Sci., Polym. Chem. Ed.* **1987**, *25*, 489.
(8) Ober, C. K.; Jin, J.-I.; Lenz, R. W. *Adv. Polym. Sci.* **1984**, *59*, 103.
(9) Dobb, M. G.; McIntyre, I. E. *Adv. Polym. Sci.* **1984**, *60/61*, 61.
(10) Noel, C.; Friedrich, C.; Bosio, L.; Strazielle, C. *Polymer* **1984**, *25*, 1281.
(11) Bosio, L.; Fayolle, B.; Friedrich, C.; Laupretre F.; Meurisse, P.; Noel, C.; Vilet, J. In *Liquid Crystals and Ordered Fluids*; Cifferi, A. C., Johnson, J. F., Eds.; Plenum: London–New York, 1984.
(12) Kricheldorf, H. R.; Pakull, R.; Buchner, S. *Polymer* **1987**, *28*, 1772.
(13) Jpn. Kokai Tokyo Koho, JP 5 891 818, May 31, 1983.
(14) Kricheldorf, H. R. *Syntheses* **1972**, 551.
(15) De Abajo, J.; Babé, S. G.; Fontán, J. *Angew. Makromol. Chem.* **1971**, *19*, 121.
(16) Mleziva, J.; Cernak, V.; Mazura, J. *Chem. Prum.* **1980**, *28*, 87; *Chem. Abstr.* **1978**, *89*, 110909y.
(17) Honoré, P.; Deltens, G.; Marechal, E. *Eur. Polym. J.* **1980**, *16*, 909.
(18) Demans, D.; Richter, L. *Textures of Liquid Crystals*; Verlag Chemie: Weinheim, 1978.
(19) Asrar, J.; Toricemi, H.; Watanabe, S.; Krigbaum, W. R.; Cifferi, A.; Preston, J. *J. Polym. Sci., Polym. Phys. Ed.* **1983**, *21*, 1119.
(20) Frosini, K.; Marchetti, A.; de Petris, S. *Makromol. Chem., Rapid. Commun.* **1982**, *3*, 795.
(21) Leadbetter, A. J.; Norris, E. K. *Mol. Phys.* **1979**, *38* 669.
(22) Kricheldorf, H. R.; Pakull, R.; Buchner, S. *J. Polym. Sci., Polym. Chem. Ed.*, submitted for publication (part 22 of this series).
(23) Krigbaum, W. R.; Ciferri, A.; Acierno, D. *J. Appl. Polym. Phys. Appl. Polym. Symp.* **1985**, *41*, 293.
(24) Krigbaum, W. R.; Watanabe, J. *Polymer* **1983**, *24*, 1299.
(25) Zentel, R.; Schmidt, G. F.; Meyer, J.; Bandia, M. *Liquid Crystals*, in press.

Preparation and Polymerization of a New Type of Stable Quinodimethanes with Captodative Substituents: 7,8-Bis(ethylthio)-, 7,8-Bis(phenylthio)-, and 7,8-Bis(*tert*-butylthio)-7,8-dicyanoquinodimethanes

Shouji Iwatsuki,* Takahito Itoh, and Ikuhiro Miyashita

Department of Chemical Research for Resources, Faculty of Engineering, Mie University, Kamihama-cho, Tsu, Japan. *Received June 24, 1987*

ABSTRACT: 7,8-Bis(ethylthio)-7,8-dicyanoquinodimethane (**3a**), 7,8-bis(phenylthio)-7,8-dicyanoquinodimethane (**3b**), and 7,8-bis(*tert*-butylthio)-7,8-dicyanoquinodimethane (**3c**) as quinodimethanes with captodative substituents were successfully prepared as stable crystals at room temperature. The first reduction potential values of **3a**, **3b**, and **3c** were measured in dichloromethane containing tetrabutylammonium perchlorate (0.1 mol/L) by cyclic voltammetry to be −0.76, −0.61, and −0.70 V, respectively. **3a** is homopolymerizable with 2,2′-azobis(isobutyronitrile) (AIBN), butyllithium, triethylamine, and boron trifluoride etherate initiators. **3b** is, even though in low level, homopolymerizable with AIBN and butyllithium but is not homopolymerizable with triethylamine and boron trifluoride etherate. **3c** is not homopolymerizable with any of these initiators.

Previously it was reported that 7,8-bis(alkoxycarbonyl)-7,8-dicyanoquinodimethanes (**1**)[1,2] and 7,8-diacyl-7,8-dicyanoquinodimethanes (**2**),[3] carrying two kinds of electron-accepting substituents at each 7 and 8 position, are obtainable as stable crystals at room temperature, are homopolymerizable with free radical and anionic initiators, the latter of which gives high polymers of **1** with a molecular weight above two million, and are copolymerizable with styrene in a random fashion. In addition, kinetic study[4] of their radical polymerizations revealed that values of entropy of polymerization for **1** and **2** are nearly constant and one-third as large as those for vinyl monomers, suggesting that those quinodimethane compounds polymerize as a new class of monomers different from vinyl and related compounds.

Recently, Viehe et al.[5] pointed out a strong resonance stabilization effect on a carbon radical carrying both electron-accepting (cyano, alkoxycarbonyl groups, etc.) and electron-donating groups (alkylthio, alkoxy groups, etc.) and called it a captodative substituent effect. Quinodimethanes carrying both captive and dative substituents at each 7 and 8 position were expected interestingly to exhibit homopolymerizability similar to **1** and **2** because of carrying different substituents at each 7 and 8 position. In addition, when a pair of captive and dative substituents are selected properly, they should change in their polar character from electron accepting to electron donating and there is the probability of obtaining a quinodimethane compound of polarity close to neutral. Furthermore they might polymerize in a peculiar manner due to the strong resonance stabilization effect, the so-called captodative substituent effect. However, those compounds have not been prepared yet.

This work describes the preparation of 7,8-bis(ethylthio)-7,8-dicyanoquinodimethane (**3a**), 7,8-bis(phenylthio)-7,8-dicyanoquinodimethane (**3b**), and 7,8-bis(*tert*-butylthio)-7,8-dicyanoquinodimethane (**3c**) as captodative substitutional quinodimethanes and their homopolymerizations.

Experimental Section

7,7,8,8-Tetrakis(ethylthio)-*p*-xylene (5a). Terephthaldehyde (**4**) (22.64 g (168.8 mmol)) and ethyl mercaptan (41.95 g (675.1 mmol)) were dissolved in 250 mL of chloroform at room temperature. Boron trifluoride etherate (10.6 mL) was added dropwise to it with stirring. After the reaction mixture was kept at room temperature for 24 h, it was dried over anhydrous magnesium sulfate and placed under reduced pressure to remove volatile material and to obtain 43.0 g of pale yellow viscous ma-

0024-9297/88/2221-0557$01.50/0 © 1988 American Chemical Society